Journal of Molecular Liquids 243 (2017) 132–143

Contents lists available at ScienceDirect

Journal of Molecular Liquids

journal homepage: www.elsevier.com/locate/molliq

Adsorptive removal of acid violet 17 dye from wastewater using biosorbent obtained from NaOH and H_2SO_4 activation of fallen leaves of *Ficus racemosa*

Suyog N. Jain, Parag R. Gogate *

Chemical Engineering Department, Institute of Chemical Technology, Nathalal Parekh Marg, Matunga, Mumbai 400019, India

ARTICLE INFO

Article history:
Received 12 June 2017
Received in revised form 1 August 2017
Accepted 3 August 2017
Available online 4 August 2017

Keywords:
Dye removal
Adsorption
Activation energy
Isotherms
Thermodynamics
Continuous operation

ABSTRACT

Biosorbents obtained from NaOH and H_2SO_4 activation of fallen leaves of *Ficus racemosa* were used for the adsorptive removal of Acid Violet 17 dye from wastewater. BET, SEM and FTIR techniques were used for the characterization of biosorbent. Batch studies were conducted to study the effect of various operating parameters on the extent of adsorption of dye. Maximum dye removal was obtained under optimized conditions of pH as 2 and 3 g/L of biosorbent dose for NaOH activated biosorbent whereas lower extent of removal was obtained for H_2SO_4 activated biosorbent under similar conditions. The obtained kinetic data were best fitted to pseudo-second order model whereas the adsorption equilibrium data was observed to be in good agreement with Langmuir model. Maximum Langmuir biosorption capacities were estimated to be 45.25, 61.35 and 119.05 mg/g for raw biosorbent, H_2SO_4 activated biosorbent and NaOH activated biosorbent respectively. The obtained thermodynamic data confirmed that adsorption was endothermic whereas the obtained activation energy as 7.07 kJ/mol confirmed physical nature of the adsorption. Column studies were also performed to establish the practical applicability of the synthesized biosorbent with understanding into effect of biosorbent bed height, initial dye concentration and flow rate. The column data for the equilibrium adsorption was observed to best fit Thomas model. Maximum biosorption capacity obtained in continuous mode under the optimized conditions was 69.08 mg/g. Batch and column desorption studies performed for five cycles established effectiveness and the reusability of synthesized biosorbent to treat industrial dye effluent effectively.

1. Introduction

Dyes are widely used as coloring agent in paper, leather, cosmetic and textile industry [1]. Due to continuous increase in demand of dyes and development of newer dye molecules, treatment of dye wastewater is becoming a serious problem [2]. Continuous discharge of dye effluents from textile industries into water bodies creates severe environmental problems as synthetic dyes are toxic and harmful to flora and fauna in water and human beings [3]. Dye effluents also create significant aesthetic problems as they give obnoxious color to the water [4]. The presence of dyes in water bodies increases chemical oxygen demand and creates hurdle for penetration of light in water bodies affecting photosynthetic activity of aquatic plants [5]. Dyes may have carcinogenic and mutagenic effect on aquatic life [6]. Even at very low concentrations, dyes may have toxic effect and are extremely difficult to remove due to their complex structure [7]. It is difficult to decolorize dye wastewater by conventional wastewater treatment methods due to the stability of dyes against heat, light and microbial attacks [8]. Hence to protect the eco-system, suitable techniques for treatment of dye bearing effluent are required to be developed.

Amongst the different available techniques, adsorption is the most widely used for the removal of dyes from wastewater due to the flexibility in operation and no generation of hazardous by-products [9]. In the adsorption, activated carbon is the most preferred adsorbent due to its high surface area, micro-porous structure, good surface reactivity and improved adsorption capacity. Activated carbon does offer problems with economics and reusability [10]. Several studies have been reported for dye removal using different adsorbents based on coal, *Aspergillus niger*, granular and powdered activated carbon [11–14]. However, the adsorption capacities have been generally lower, the production costs for materials are higher and some of the reported adsorbents from materials like *Aspergillus niger* and activated carbon also suffer from limitation of effective regeneration. These facts have motivated researchers to develop other sustainable adsorbents especially those which can be obtained from waste materials with some form of activation. The present study aimed at biosorbent synthesis from fallen *Ficus racemosa* (FR) leaves, an agricultural waste and application of synthesized biosorbent for adsorptive removal of Acid Violet 17 (AV 17) dye from wastewater. Agricultural waste based biomass has been selected as a raw material

* Corresponding author.
E-mail address: pr.gogate@ictmumbai.edu.in (P.R. Gogate).

http://dx.doi.org/10.1016/j.molliq.2017.08.009
0167-7322/

for synthesis of biosorbent in the present work due to the widespread availability in nature and considering the fact that any use of such waste biomass can reduce volume of solid waste to be treated. The synthesis of biosorbent also includes the use of activation methods with an objective to increase porosity and surface area of the synthesized biosorbent as well as impart additional functional groups, which can improve the biosorption capacities. In the present study, biosorbent has been synthesized from the fallen leaves of FR in the natural form and with activation using NaOH and H_2SO_4. The study also aimed to investigate the effects of pH, biosorbent dosage, time, AV 17 dye concentration and temperature on the extent of adsorption in batch operation. The practical applicability of synthesized biosorbent on commercial scale has also been confirmed using studies based on the column operation. In the continuous column operations, the effects of biosorbent bed height, initial AV 17 dye concentration and dye flow rate on the extent of dye removal have been investigated and breakthrough parameters were established to obtain the important information for column design.

2. Materials and methods

2.1. Synthesis of biosorbent

2.1.1. NaOH activated biosorbent

Fallen FR leaves were collected from Nashik, India. Collected biomass was washed, crushed and sieved to obtain particle size range of 53–106 μm. Lignin from fallen leaves of FR powder was removed by impregnation with 1% (weight) solution of NaOH in the ratio of 1:5. Detailed process of biosorbent synthesis using NaOH activation of FR has been given in our earlier work [15]. The synthesized NaOH activated FR biosorbent was then kept in desiccator and used for further experiments.

2.1.2. H_2SO_4 activated Ficus racemosa

One part of dried fallen leaves of FR powder was mixed with one part of concentrated H_2SO_4 solution and solution was heated at 353 K for 18 h. Resulting material was then soaked in 1% $NaHCO_3$ solution to remove residual acid and dried in oven for 6 h. The obtained H_2SO_4 activated FR was also kept in desiccator and used for further experiments.

2.2. Pollutant dye

Acid violet 17 [Molecular formula = $C_{41}H_{44}N_3NaO_6S_2$], an anionic dye was purchased from Sigma-Aldrich, Mumbai, India. The dye was dark violet in color. The stock solution of dye (1 g/L) was prepared and subsequently diluted to get the dye solutions of desired concentrations required in the study.

2.3. Instruments and analysis method

Scanning electron microscope (SEM, JEOL, USA) was used to determine morphological features and surface characteristics of NaOH activated and H_2SO_4 activated FR biosorbents. The Fourier transform infrared spectroscopy (FTIR, Perkin Elmer, USA) was also performed to determine the functional groups present on the biosorbent that can be efficiently involved in the adsorption of AV 17 on activated FR biosorbent. BET parameters of biosorbents were determined using the Brunauer-Emmett-Teller (PMI BET Sorptometer, USA) analysis.

UV–visible Spectrophotometer (UV 1800, Shimadzu) was used for the quantification of the concentration of AV 17 dye by recording the absorbance at λ_{max} of 543 nm. Calibration curve of AV 17 was constructed and linear behavior between absorbance and concentration was observed with correlation coefficient, R^2 value of 0.9994. Limit of detection (LOD) and limit of quantification (LOQ) values were obtained from slope of the calibration curve and standard deviation. LOD and LOQ values were obtained as 0.037 and 0.124 mg/L respectively for AV 17 dye.

2.4. Batch biosorption methodology

Batch experiments were conducted in orbital shaking incubator (Bio-Technics, India) by adding known quantity of biosorbent in 50 mL of known concentration of AV 17 dye at the required pH value. The speed of the shaker was maintained at 150 rpm. The pH was maintained at the required value by addition of acid/alkali. Different operating parameters such as pH, biosorbent dose, time, initial dye concentration and temperature were varied to study the effect on dye removal. Dye concentration in supernatant samples was determined using UV spectrophotometer. Desorption studies were performed to regenerate spent biosorbent. During the analysis, biosorption capacity, q_t (mg/g) at any time t (min) was determined using following equation:

$$q_t = \frac{(C_i - C_t)}{m} \tag{1}$$

Where C_i and C_t are initial dye concentration and concentration of dye at any time t, respectively (mg/L) and m is biosorbent dose (g/L).

The extent of dye removal expressed as percentage was also calculated using the following equation:

$$\text{Dye removal } (\%) = \frac{C_i - C_t}{C_i} \times 100 \tag{2}$$

2.5. Column biosorption methodology

Continuous experiments of biosorption were also conducted in a column with 20 mm as inner diameter, 24 mm as the outer diameter and height as 250 mm. The biosorbent bed was supported with glass beads. Column was packed with glass wool to avoid loss of biosorbent. Packing density of the biosorbent bed was estimated to be 0.4972 g/cm^3. Column was operated in an up flow mode. Acid violet 17 solution of required concentration and pH 2 was passed though the column in upward direction using peristaltic pump (Ravel Hiteks, India). Different experiments were conducted to study the effect of biosorbent bed height, initial concentration of dye and flow rate on the extent of dye removal. Desorption studies were conducted for the regeneration of bed and subsequent reuse till five cycles. Breakthrough curves (plot of Ct/Ci against time, where C_t is the concentration of dye in the outlet from column at time t (min) and C_i is the inlet concentration) were plotted and fitted to various adsorption models. Different design parameters were determined from the breakthrough curve analysis as per the following process:

Breakthrough time (t_b) was determined as the time when $Ct/Ci = 0.1$ and exhaustion time (t_e) was determined as the time when $Ct/Ci = 0.9$ [16].

The treated volume of effluent, V_e was determined using the following equation:

$$V_e = Ft_e \tag{3}$$

Where F is flow rate of dye solution (mL/min).

Total adsorbed quantity of the dye, q_{ads} (mg) in the column for given feed conditions was calculated using the following equation [17]:

$$q_{ads} = \frac{F}{1000} \int_{t=0}^{t=t_{total}} C_{ads} dt \tag{4}$$

where C_{ads} is the adsorbed dye concentration on the biosorbent (mg/L) calculated from the difference between inlet and outlet dye concentration and t_{total} is total time of operation (min).

The experimental maximum adsorption column capacity, q_m (mg/g) was determined using the following equation [18]:

$$q_m = \frac{q_{ads}}{M} \tag{5}$$

Where q_{ads} (mg) is dye adsorbed on the biosorbent and M is quantity of biosorbent in the column (g).

Desorption efficiency (E) described as the ratio of dye desorbed from biosorbent (q_{des}) to dye adsorbed on the biosorbent (q_{ads}) was determined using the following equation [19]:

$$E(\%) = \frac{q_{des}}{q_{ads}} \times 100 \tag{6}$$

Model fitting of the experimental data was analyzed in terms of sum of square error (SSE) function to determine the best model fitting for the obtained column data. SS error values were also determined using the following equation [20]:

$$SSE = \frac{\sum \left[\left(\frac{C_t}{C_i}\right)_c - \left(\frac{C_t}{C_i}\right)_e \right]^2}{n} \tag{7}$$

Where $(C_t/C_i)_c$ is the ratio of concentration of dye in the outlet at time t to concentration of dye in the inlet, determined from equation of a model and $(C_t/C_i)_e$ is the same ratio determined experimentally and n is number of experimental points used for the specific operating conditions.

3. Results and discussion

3.1. Biosorbent characterization

Fig. 1 depicts the scanning electron microscopy images of synthesized NaOH activated FR and H_2SO_4 activated FR biosorbents before and after the use in the adsorption of acid violet. The images depicted in Fig. 1a and Fig. 1c for biosorbent before adsorption shows that both the biosorbent have number of cavities and pores which confirm favorable adsorption characteristics. The surface of the biosorbents also seems to be irregular and uneven with cavities (more open in the case of NaOH activated FR) which can facilitate interaction of dye ions with the biosorbent surface leading to favorable dye adsorption. An alteration in rough biosorbent surfaces (Fig. 1b and Fig. 1d) was observed after the use in the adsorption confirming the proposed mechanisms of favorable dye interactions leading to adsorption of dye on NaOH activated FR and H_2SO_4 activated FR biosorbents.

Fig. 2a and b depicts the results for the FTIR analysis of the NaOH activated FR biosorbent before and after dye adsorption. The peak at 3444 cm^{-1} indicates the presence of –OH and/or –NH groups on NaOH activated FR biosorbent, which is shifted to 3453 cm^{-1} after adsorption of dye. The peak at 1622 cm^{-1} can be attributed to carboxylic group of the biosorbent, which is shifted to 1614 cm^{-1} in the image of biosorbent after use confirming the dye adsorption on biosorbent [21]. The peak at 1020 cm^{-1} can be due to C—O—C stretching of cellulose which is shifted to 1017 cm^{-1} after dye adsorption [22]. The peak at 2925 cm^{-1} can be due to C—H stretching vibration [23,24]. The two new peaks at 1281 cm^{-1} attributed to C—N stretch and 1180 cm^{-1} attributed to SO stretch of AV 17 dye appearing in Fig. 2b also confirmed the dye adsorption [25].

BET surface area, pore diameter and pore volume of fallen leaves of FR, H_2SO_4 activated FR and NaOH activated FR have been summarized in Table 1. BET surface area was obtained as 21.177 m^2/g for the fallen leaves of FR, which was increased to 41.796 for H_2SO_4 activated FR and to 136.257 m^2/g for the case of NaOH activated FR. Typically, NaOH and H_2SO_4 treatment helps in removal of lignin from the biomass, which gives a bound structure to the biomass and can interfere with the adsorption of the dye on the biosorbent. Both the treatments applied in the present study also developed pores and thus increased porosity of the biosorbent and hence the surface area (as seen from data shown in Table 1), which are favorable characteristics for dye adsorption. It was also established that the surface area obtained by NaOH treatment to fallen leaves was more than that obtained due to the H_2SO_4 treatment.

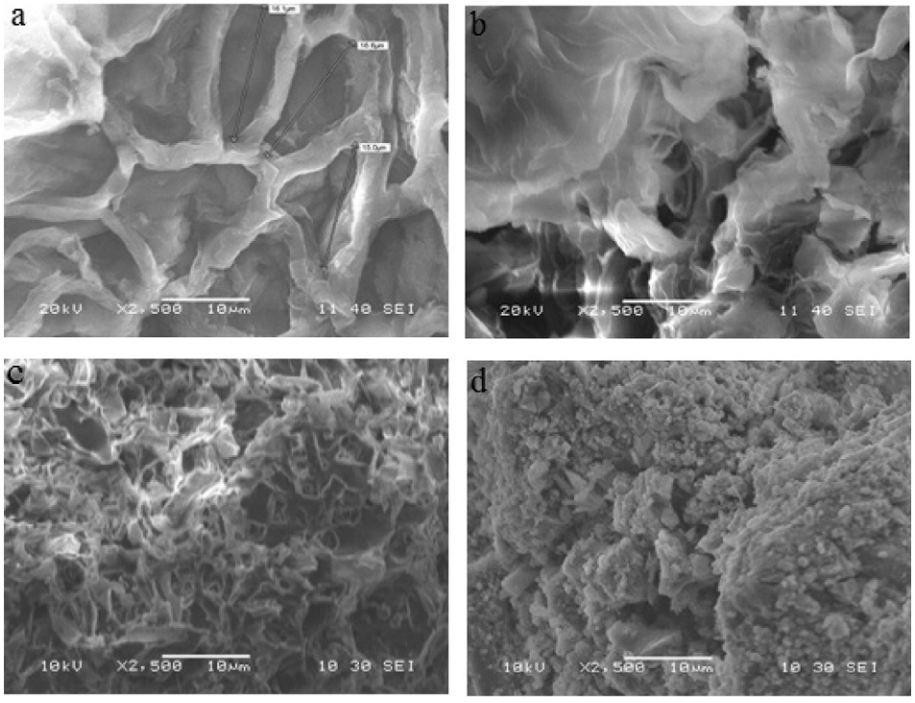

Fig. 1. Scanning electron microscopy images of NaOH activated FR (a) before dye adsorption (b) after dye adsorption and H_2SO_4 activated FR (c) before dye adsorption (d) after dye adsorption.

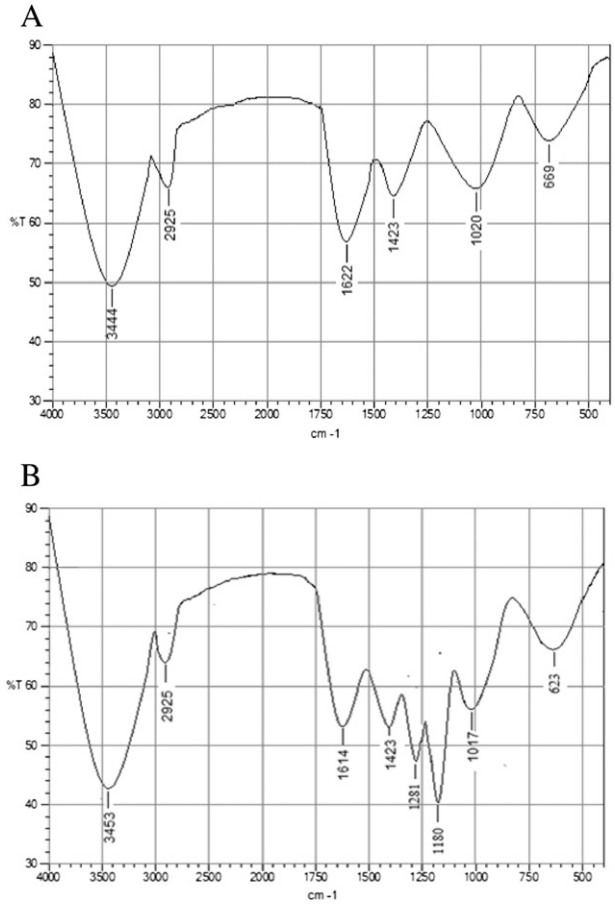

Fig. 2. a FT-IR spectra of NaOH activated FR before dye adsorption. **b** FT-IR spectra of NaOH activated FR after dye adsorption.

3.2. Batch studies

3.2.1. Effect of pH

The effect of pH on the removal of AV 17 dye using NaOH activated FR biosorbent (considering the higher biosorption capacity as per the results of surface area) was studied over the range of 2 to 10 and obtained results are depicted in Fig. 3. It can be seen from Fig. 3 that extent of AV 17 dye removal increased from 28.73% to 96.42% with a decrease in pH of the dye solution from 10 to 2. The biosorption capacity (q_t) also increased from 7.18 to 24.11 mg/g with a decrease in pH of the dye solution from 10 to 2. AV 17 carries negative charge in an aqueous solution due to the presence of sulphonate group and hence it is necessary to have positive charge on the biosorbent surface for effective dye removal. Under the acidic conditions (pH of 2), H^+ ions concentration is significantly higher in the system giving the maximum positive charge on the surface of biosorbent leading to maximum removal of anionic AV 17 dye based on the favorable electrostatic attractions [26,27]. Similar trend was also reported for removal of reactive blue dye 5G using the polymeric adsorbent, Dowex Optipore SD-2 [28] and for the case of Congo red using the cationic modified orange peel powder as the biosorbent [1].

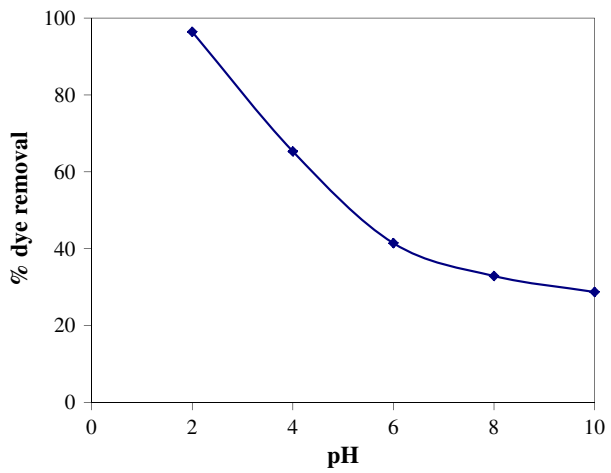

Fig. 3. Effect of pH on removal of AV 17 using NaOH activated FR ($T = 303$ K, $t = 240$ min, $C_i = 100$ mg/L, $m = 3$ g/L).

3.2.2. Effect of biosorbent dose (m)

Fig. 4 shows the obtained results for the experiments related to understanding the biosorbent dose effect on AV 17 dye removal using NaOH activated FR and H_2SO_4 activated FR biosorbent. Biosorbent dosage in the present study was varied from 0.5 to 5 g/L for NaOH activated FR biosorbent and from 1 to 10 g/L for H_2SO_4 activated FR biosorbent (considering expected lower capacity for H_2SO_4 based biosorbent) . It has been observed that the extent of dye removal (%) increased significantly from 28.87% at 0.5 g/L loading to 96.42% at 3 g/L for the case of NaOH activated FR biosorbent and from 43.61% at 1 g/L loading to 86.30% at 5 g/L for the case of H_2SO_4 activated FR biosorbent. Beyond the optimum loadings for each biosorbent, dye removal is only slightly increased with increase in loading from 3 to 5 g/L for NaOH activated FR and from 5 to 10 g/L for H_2SO_4 activated FR. The marginal changes in the dye removal after 3 g/L loading for NaOH activated FR and 5 g/L loading for H_2SO_4 activated FR can be attributed to possible aggregation of sites available for adsorption [8] and hence dye adsorption is not affected significantly. The observed optimum dose of 3 g/L for NaOH activated FR and 5 g/L for H_2SO_4 activated FR was used for subsequent experimentation. Similar trend in terms of existence of optimum has been reported for the adsorption of methyl orange using surfactant modified coffee waste [29]. The obtained results in the present work also indicated better dye removal results at lower dose for NaOH activated FR biosorbent as compared to the H_2SO_4 activated FR biosorbent, which can be attributed to the higher surface areas as established using the BET surface area analysis. It was also observed in the present work that an increase in the biosorbent dose caused a decrease in biosorption capacity (q_t) as it can be seen from Eq. 1 that q_t is inversely proportional to biosorbent dose. Similar nature has also been reported for the adsorption of Reactive Red 194 and Direct Blue 53 onto biosorbent obtained from cupuassu shell [30].

3.2.3. Effect of contact time (t)

Fig. 5 shows the results for the effect of contact time on dye removal using NaOH activated FR biosorbent at 50, 100 and 200 mg/L of AV 17 dye concentrations. The dye removal was much faster in first 30–

Table 1
BET surface area, pore volume and pore diameter of fallen leaves of FR, H_2SO_4 activated FR and NaOH activated FR.

Adsorbent sample	Surface area (m^2/g)	Total pore volume (cm^3/g)	Average pore diameter (nm)
Fallen leaves of FR	21.177	0.066	12.50
H_2SO_4 activated FR	41.796	0.109	10.44
NaOH activated FR	136.257	0.209	6.12

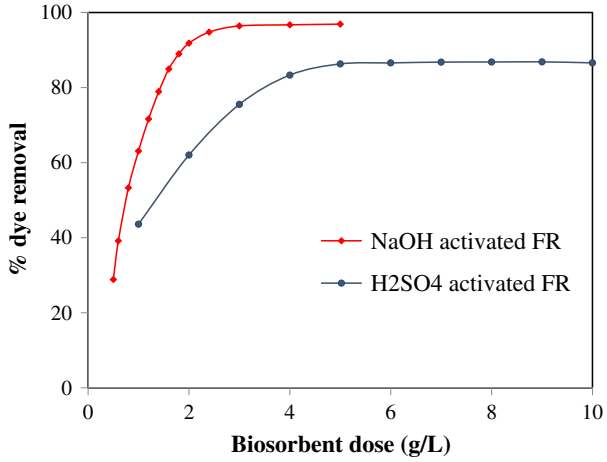

Fig. 4. Effect of biosorbent dose on removal of AV 17 using NaOH and H_2SO_4 activated FR ($T = 303$ K, $t = 240$ min, $C_i = 100$ mg/L, $pH = 2$).

60 min of contact time and later, a gradual decrease in the adsorption rate was noticed with equilibrium obtained in about 240 min. The kinetic experiments for all the dye concentrations were performed till a contact time of 360 min and negligible increase in the dye removal was noticed when contact time increased from 240 to 360 min. Hence treatment time of 240 min has been selected as the time required to reach equilibrium and the subsequent experiments of adsorption were conducted for a contact time of 240 min. Similar trend has been observed for the adsorption of crystal violet dye onto chitosan composite [31]. The faster dye removal in the initial period of adsorption is attributed to more number of empty sites being available on the biosorbent for dye adsorption whereas in the later stages, gradually exterior biosorbent surface gets exhausted reducing the quantum of the sites available for adsorption and hence removal rate is decreased in the later period of adsorption, which is also a typical behavior observed for equilibrium type systems [32].

3.2.4. Effect of initial dye concentration (Ci)

Fig. 5 also shows the results for the effect of initial dye concentration (C_i) on AV 17 dye removal and obtained kinetic parameters based on the

Table 2
Kinetic parameters for removal of AV 17 using NaOH activated FR ($T = 303$ K, $t = 360$ min, $pH = 2$, $m = 3$ g/L).

Kinetic model	Parameter	Values		
Pseudo first-order	C_i (mg/L)	50	100	200
	q_{exp} (mg/g)	16.51	32.25	60.87
	q_e (mg/g)	9.95	29.17	50.49
	k_f (min^{-1})	0.0358	0.0235	0.0194
	R^2	0.9743	0.9582	0.9610
Pseudo second-order	C_i (mg/L)	50	100	200
	q_{exp} (mg/g)	16.51	32.25	60.87
	q_e (mg/g)	16.92	33.78	64.94
	k_s (g mg^{-1} min^{-1})	0.0097	0.0020	0.0008
	h (mg/g min^{-1})	2.78	2.33	3.24
	R^2	0.9997	0.9996	0.9994
Elovich	C_i (mg/L)	50	100	200
	α (mg/g min^{-1})	270.91	40.44	25.26
	β (g mg^{-1})	0.63	0.24	0.11
	R^2	0.8411	0.9659	0.9769
Weber-Morris	C_i (mg/L)	50	100	200
First stage	K_{ip} (mg/g $min^{-1/2}$)	0.83	1.78	3.24
	I (mg/g)	8.41	13.05	21.72
	R^2	0.9806	0.9836	0.9936
Second stage	K_{ip} (mg/g $min^{-1/2}$)	0.02	0.83	1.56
	I (mg/g)	16.18	20.62	37.71
	R^2	0.4523	0.9970	0.9769
Third stage	K_{ip} (mg/g $min^{-1/2}$)	–	0.11	0.17
	I (mg/g)	–	30.34	57.73
	R^2	–	0.7548	0.7840

trends are shown in Table 2. The biosorption capacity (q_t) values were estimated to be 16.92, 33.78 and 64.94 mg/g for dye concentration of 50, 100 and 200 mg/L, respectively. Similar trend of increase in biosorption capacity with an increase in dye concentration has also been reported for the removal of Acid Blue 113 using surfactant modified *Prunus dulcis* [33]. The extent of dye removal decreased from 99.04% at 50 mg/L of dye concentration to 90.36% at 200 mg/L of dye concentration. At lower dye concentrations, all dye molecules interact with the biosorbent sites resulting in maximum dye removal whereas at higher dye concentrations, all dye molecules are not getting adsorbed on sites and some of the dye molecules remain unadsorbed due to the competition with the active sites resulting in a decrease in the extent of dye removal. It is also important to understand that the quantity of dye removed per unit adsorbent increased with an increase in the initial

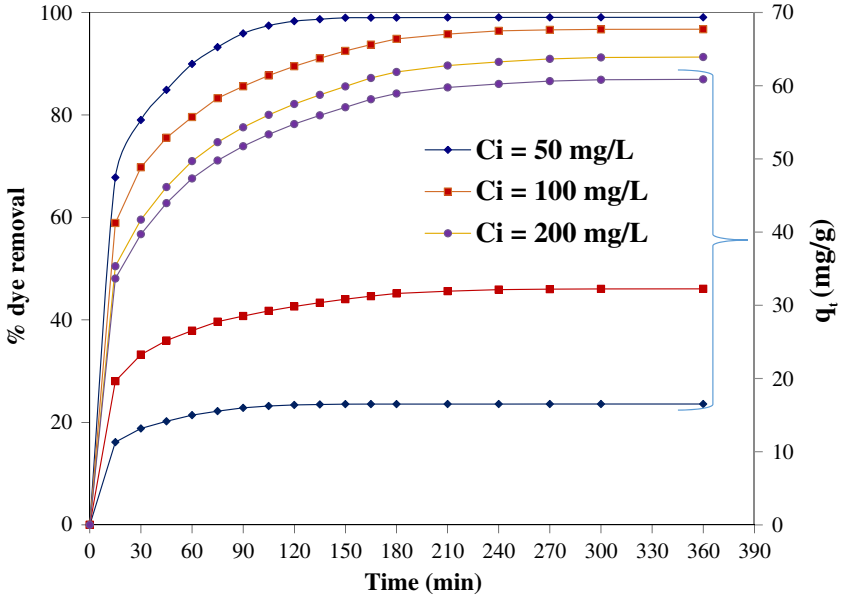

Fig. 5. Effect of contact time and initial dye concentration on removal of AV 17 and biosorption capacity of NaOH activated FR ($T = 303$ K, $C_i = 50$–200 mg/L, $pH = 2$, $m = 3$ g/L).

concentration, which is an important design information. Similar nature of the trend in variation has been reported for the removal of methylene blue using the cellulose grafted with soy protein isolate [34] as well as domestic waste [35].

3.2.5. Adsorption kinetics

For understanding the mechanism of the adsorption, it is important to process the adsorption kinetic data and obtain the kinetic parameters as order and rate constant using different models [36]. Several kinetic models are available to describe the mechanism of adsorption. In present study, kinetics of adsorption of AV 17 was fitted into four kinetic models namely pseudo first-order, pseudo second-order, Elovich and Weber-Morris intra-particle diffusion model.

3.2.5.1. Pseudo first-order model: The linearized form of equation for pseudo first-order model is given as follows [37]:

$$log(q_e - q_t) = -\frac{k_f t}{2.303} + log q_e \quad (8)$$

where, q_e is biosorption capacity at equilibrium (mg/g) and k_f is rate constant of pseudo first-order model (min^{-1}).

Obtained model parameters (k_f and q_e) values have been depicted in Table 2. It can be seen from the data reported in Table 2 that the correlation coefficient (R^2) values deviate from unity and calculated $q_{e,}$ values are also significantly different from the experimental, q_{exp} values for all the studied concentrations, which suggests that experimental data is not accurately fitted into pseudo first-order model.

3.2.5.2. Pseudo second-order model: In pseudo second-order model [38], rate of adsorption is assumed to be proportional to square of number of sites that are unoccupied. The linearized equation for pseudo second-order model is given as follows:

$$\frac{t}{q_t} = \frac{t}{q_e} + \frac{1}{k_s q_e^2} \quad (9)$$

Where k_s is rate constant of pseudo second-order model (g mg $^{-1}$ min^{-1}).

The initial rate of biosorption, h (mg g $^{-1}$ min^{-1}) is given as follows [39]:

$$h = k_s q_e^2 \quad (10)$$

The graph of t/q_t versus t has been plotted in Fig. 6 A and it can be seen that linear nature of plot is obtained for all the studied dye concentrations. The obtained model parameter (k_s, q_e and h) values have been summarized in Table 2. The correlation coefficient (R^2) values were found closer to unity and calculated $q_{e,}$ and experimental, q_{exp} values were also very close to each other for all the studied concentrations. These findings confirmed very good fitting of pseudo second-order equation to the obtained experimental data. Similar trend has also been reported for the adsorption of reactive red dye using textile sludge [6] and Congo red dye using the pineapple plant stem [40] based adsorbents. It can also be seen from Table 2 that q_e value increased significantly from 16.92 mg/g at 50 mg/L to 64.94 mg/g at 200 mg/L similar to the experimental observations as discussed earlier. Similar trend has been reported for adsorption of acid blue 25 dye on waste tea activated carbon [41] and methylene blue using activated date pits [42] based adsorbents.

3.2.5.3. Elovich model: Elovich model is used to describe chemisorption of adsorbate on adsorbent and the linearized equation for Elovich model is given as follows [43]

$$q_t = \frac{1}{\beta} \ln(\alpha\beta) + \frac{1}{\beta} \ln(t) \quad (11)$$

Where β is Elovich constant (g mg^{-1}) and α is initial rate of adsorption (mg/g min^{-1}). The model constants, β and α were determined from plot of q_t versus ln (t) for all the studied dye concentrations and obtained values are summarized in Table 2. It was observed that linear fitting was not obtained for Elovich plots (Fig. 6B) and R^2 values of Elovich model (average value 0.928) were not very close to unity indicating that Elovich model did not fit to the obtained experimental data, which also confirmed that the chemisorption is not controlling form of mechanism governing the adsorption. Similar nature was also reported for adsorption of brilliant green dye on rice husk ash [44].

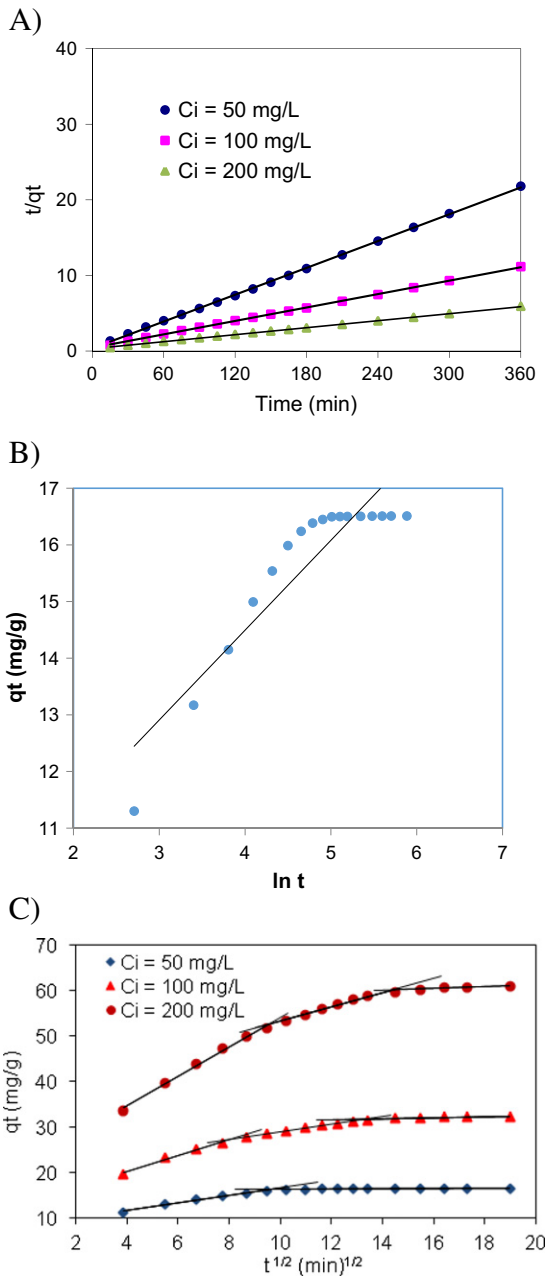

Fig. 6. Fitting of the kinetic models to the obtained batch data for removal of AV 17 using NaOH activated FR under conditions of $T = 303$ K, $pH = 2$, $m = 3$ g/L A) Pseudo-second order plot B) Elovich plot C) Weber-Morris intra-particle diffusion plot.

3.2.5.4. Weber-Morris diffusion model: Weber-Morris model is the widely used intra-particle diffusion model to predict the rate determining step in the overall adsorption process and is mathematically expressed as follows [45]:

$$q_t = k_{ip} t^{0.5} + I \quad (12)$$

Where k_{ip} is the rate constant (mg/g $min^{-1/2}$) determined from the slope and I is the constant of model (mg/g) determined from the intercept of the plots of q_t against $t^{0.5}$. The values of the model parameters decide the controlling mechanisms in the adsorption. In present study as seen from Fig. 6C, the plots for all the concentrations do not pass through the origin indicating some degree of control from the boundary layer and also other mechanisms in addition to the intra-particle diffusion [29,46]. The intra-particle diffusion plot in present study shows involvement of two-three stages. The first stage involves faster diffusion of dye through the boundary layer of solution to the external surface of NaOH activated FR, commonly described as the external surface adsorption. The second stage involves gradual adsorption where controlling mechanism of intra-particle diffusion is rate determining step. In third stage, concentration of dye in the solution is very low and hence intra-particle diffusion begins to drop and this stage indicates attainment of equilibrium [35]. Similar three stage characteristics have been reported for the adsorption of methylene blue on cellulose grafted with soy protein isolate [34] whereas two stages in intra-particle diffusion model were reported for adsorption of crystal violet on citric acid activated wheat straw [47] based biosorbent. The existence of two or three stages depends on the type of system and the operating conditions in terms of concentration. In the present work, it has been observed from Fig. 6C that only two stages are involved for 50 mg/L of dye concentration whereas three stages are involved for the remaining dye concentrations. The values of slope, k_{ip} and intercept, I obtained for all the stages are depicted in Table 2. The values of rate constant, k_{ip} were found to increase with an increase in dye concentration from 50 to 200 mg/L, which is due to enhanced driving force available at higher dye concentrations [48]. The intercept I in the plot represents boundary layer thickness. Typically higher I values indicate greater effect of boundary layer [49]. It can be seen from Table 2 that value of I in all stages for all studied dye concentrations is found to increase with an increase in the concentration confirming higher contribution of the boundary layer at higher concentrations.

3.2.6. Effect of temperature

Fig. 7 illustrates the effect of temperature (293–323 K) on the biosorption capacity. It was observed that the equilibrium curves are initially steeper for all the studied temperatures and became flatter in later stages indicating saturation of the biosorbent with time, again a typical equilibrium characteristics. It can be also seen from the plot that the biosorption capacity increased with temperature and maximum biosorption capacity was obtained at temperature of 323 K. An increase in temperature from 293 to 323 K led to a corresponding increase in maximum Langmuir biosorption capacity from 106.38 to 119.05 mg/g. Similar trend has also been reported for the adsorption of basic blue 41 on activated local clay material [50]. The observed trend may not be generalized as in some cases such as adsorption of sunset yellow dye using modified Iron stick yam skin [51] and basic red 46 dye using molasses modified boron enrichment waste [52], lower temperatures has been reported to favor adsorption. Thus, it is important to establish the effect of temperature on the specific dye in question and the methodology presented in the work can be useful.

Table 3
Isotherm parameters for removal of AV 17 using NaOH activated FR ($t = 240$ min, $pH = 2$, $m = 3$ g/L).

Isotherm model	Parameter	Values			
Langmuir	T (K)	293	303	313	323
	K_L (L/mg)	0.073	0.081	0.093	0.111
	q_{max} (mg/g)	106.38	111.11	114.94	119.05
	R^2	0.9952	0.9949	0.9949	0.9959
Dubinin–Radushkevich	T (K)	293	303	313	323
	q_{max} (mg/g)	71.24	73.27	75.55	77.78
	E (kJ/mol)	1.31	1.62	1.85	2.07
	R^2	0.6402	0.636	0.6339	0.6333
Temkin	T (K)	293	303	313	323
	K_T (L/mg)	2.36	3.00	3.47	3.99
	B_T (mg/g)	16.25	16.40	16.99	17.64
	R^2	0.9649	0.9633	0.966	0.9694

3.2.7. Adsorption equilibrium study

Adsorption equilibrium data obtained in the present study was analyzed using three isotherm models viz. Langmuir, Dubinin–Radushkevich and the Temkin.

Langmuir model [53] assumes monolayer sorption of solute on adsorbent with constant energy of adsorption. The linear equation of the model is as follows:

$$\frac{C_e}{q_e} = \frac{C_e}{q_{max}} + \frac{1}{q_{max} K_L} \quad (13)$$

Where q_{max} is maximum Langmuir monolayer capacity (mg/g) and K_L is Langmuir model constant (L/mg).

Dubinin–Radushkevich isotherm model [54] is applied to describe adsorption on porous adsorbents. The linear equation of the model is

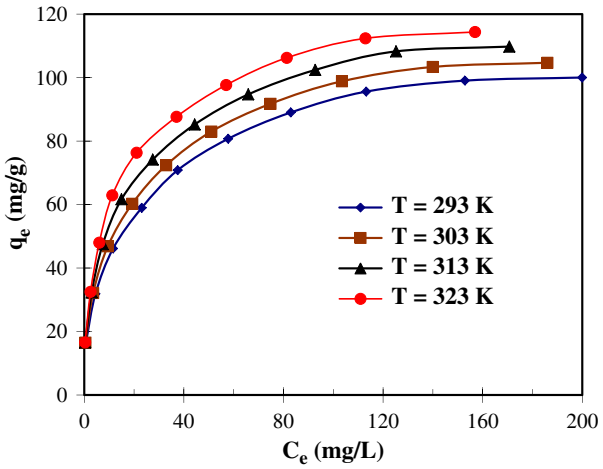

Fig. 7. Effect of temperature on the removal of AV 17 using NaOH activated FR ($t = 240$ min, $pH = 2$, $m = 3$ g/L).

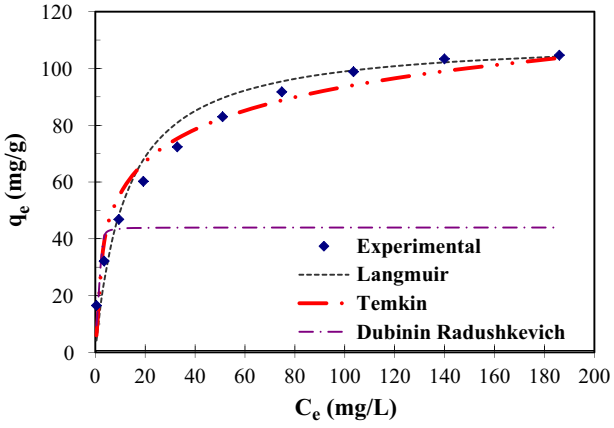

Fig. 8. Comparison of $q_{e,exp.}$ with $q_{e,cal}$ from various isotherm models for removal of AV 17 using NaOH activated FR ($t = 240$ min, $pH = 2$, $m = 3$ g/L).

Table 4
Thermodynamic parameters for removal of AV 17 using NaOH activated FR biosorbent at different temperatures.

Isotherm model	ΔG^0 (kJ/mol)				ΔH^0 (kJ/mol)	ΔS^0 (kJ/mol K)
	293 K	303 K	313 K	323 K		
Langmuir	−26.612	−27.799	−29.076	−30.466	10.98	0.13
Temkin	−35.081	−36.884	−38.481	−40.084	13.61	0.17

as follows:

$$\ln q_e = -B\varepsilon^2 + \ln q_{max} \quad (14)$$

Where q_{max} is Dubinin–Radushkevich maximum adsorption capacity (mg/g), ε is Polanyi potential (kJ/mol) and B is isotherm constant (mol^2/kJ^2) obtained from the free energy of biosorption, E (kJ/mol) as per the following equation:

$$E = \frac{1}{(2B)^{0.5}} \quad (15)$$

Temkin [55] considered the effect of interaction of adsorbate on the adsorption process. The linear equation of the model is as follows:

$$q_e = B_T \ln c_e + B_T \ln K_T \quad (16)$$

Where K_T (L/mg) is Temkin constant indicating affinity of adsorption and B_T (mg/g) corresponds to heat of adsorption.

The obtained values of the correlation coefficient, R^2 and isotherm model constants for all the three isotherms are summarized in Table 3. R^2 values for Dubinin–Radushkevich are significantly deviating from unity. The fitting of the obtained experimental data to Langmuir, Dubinin–Radushkevich and Temkin model at different temperatures in present study have been given in Fig. 8 in the form of comparison of $q_{e,cal}$ values obtained from various isotherm models with $q_{e,\exp}$. It can be seen that $q_{e,\exp.}$ values for maximum number of points are closer to $q_{e,cal}$ values obtained by Langmuir model as compared to other isotherm models. R^2 values of Langmuir model (average value 0.9952) are also found to be closer to unity as compared to other isotherms. These observations indicated that Langmuir model is in good agreement to the isotherm data obtained in the present work. The constant, K_L of Langmuir model indicates energies of interaction between AV 17 dye and adsorption sites of NaOH activated FR biosorbent [50]. As seen from Table 3, K_L values increased from 0.073 to 0.111 L/mg for an increase in temperature from 293 K to 323 K and maximum Langmuir biosorption capacity, q_{max} increased from 106.38 mg/g at 293 K to 119.05 mg/g at 323 K. These observations confirmed favorable adsorption at higher temperatures showing that adsorption process studied in the present work is endothermic in nature.

3.2.8. Adsorption thermodynamics

Feasibility and nature of the biosorption in terms of spontaneity can be established based on the Van't Hoff equation and thermodynamic calculations to quantify the Gibb's free energy change, ΔG^0 (kJ/mol), enthalpy change, ΔH^0 H^0(kJ/mol) and entropy change ΔS^0 (kJ/mol K) [18]. The calculated values of ΔG^0, ΔH^0 and ΔS^0 have been depicted in Table 4. Negative values of ΔG^0 obtained in the present study indicated spontaneous nature and feasibility of the biosorption of AV 17 on NaOH activated FR biosorbent. Values of ΔG^0 were found to be more negative at increased temperatures which shows that process is more spontaneous in nature at higher temperatures [8]. ΔH^0 value is found to be 10.98 kJ/mol confirming that the adsorption of AV 17 on NaOH activated FR is endothermic in nature [56]. As the value was lower than 40 kJ/mol, dominance of physical adsorption has also been confirmed [57]. Positive values of ΔS^0 also implied increased randomness and affinity of AV 17 dye toward NaOH activated FR biosorbent [58].

3.2.9. Activation energy calculations

Arrhenius equation [59] has been used to determine the activation energy for biosorption of AV 17 on NaOH activated FR biosorbent. E_a is energy of activation (kJ/mol). Value of E_a is generally used to determine the type of adsorption. Low activation energies (5–40 kJ/mol) indicate physical adsorption as it involves weaker forces whereas high activation energies (40–800 kJ/mol) indicate chemical adsorption as it involves stronger forces than physical adsorption [60]. In present study, activation energy has been obtained as 7.07 kJ/mol indicating that adsorption of acid violet 17 on NaOH activated FR is physical in nature.

3.2.10. Comparison with other adsorbents

To establish the potential of NaOH activated FR for AV 17 dye removal from wastewater, the obtained maximum adsorption capacities in the present study have been compared with q_{max} values of some of the more commonly reported biosorbents in the literature for acidic dye removal in general (Table 5). The data in Table 5 established that NaOH activated FR biosorbent has comparatively higher q_{max} value, 119.05 mg/g, at similar loading or adsorbent and acidic conditions in most cases, compared with the other commonly used adsorbents for different acidic dyes. The obtained results confirmed the excellent potential of NaOH activated FR biosorbent to remove AV 17 dye from wastewater with much higher adsorption capacities in comparison with commonly used adsorbents.

3.2.11. Desorption and regeneration studies

In actual wastewater treatment plants, potential applicability of the adsorbent depends on type of the adsorbent in terms of the maximum

Table 5
Maximum adsorption capacity (q_{max}) for removal of various anionic/acidic dyes from aqueous solution using different adsorbents.

Anionic dyes	Adsorbents	q_{max}(mg/g)	pH	Adsorbent dose (g/L)	Reference
Acid violet 17	NaOH activated FR	119.05	2	3	Present study
Acid violet 17	H_2SO_4 activated FR	61.35	2	5	Present study
Acid violet 17	Orange peel	19.88	2	12	[71]
Acid blue 25	*Azolla pinnata*	50.5	2	2	[72]
Acid blue 25	Soya bean waste	38.3	2	2	[72]
Acid blue 25	Activated pericarp of pecan	28.75	9	8	[73]
Acid blue 62	Colemanite ore waste	48.89	1	2	[74]
Acid orange 7	Activated Stoechospermum marginatum	71.05	2	1	[21]
Methyl orange	Surfactant modified coffee waste	62.5	3.5	2	[29]
Methyl orange	Graphene oxide	16.83	3	1	[75]
Methyl orange	Activated *Ficus carica* fiber	51.55	4	5	[76]
Reactive blue 5G	Orange baggase	34.89	2	1	[77]
Reactive blue 250	Modified natural zeolite	58.5	7	5	[78]
Congo red	β-cyclodextrin based polymer	36.2	5.8	2.5	[79]
Congo red	Coir pith	6.7	2	4	[80]
Congo red	Jute fiber	29.7	3.91	2.04	[5]

adsorption capacity and possibility of regeneration of the spent adsorbent as these factors strongly influence the economic feasibility. Hence it is necessary to study the reuse of the adsorbent after adsorption. In present study, distilled water at alkaline pH is selected as the regeneration medium. Reusability study was performed using 100 mg/L of AV 17 and NaOH activated FR for five cycles at 303 K. Desorption of dye was carried out with alkaline distilled water in orbital shaker for 30 min. At alkaline pH, electrostatic interaction between acidic AV 17 loaded spent biosorbent surface and distilled water led to faster dye desorption from spent biosorbent.

The obtained results for the adsorption capacity and desorption efficiency in five consecutive cycles revealed that adsorption capacity drops slightly by <2% for operation from first cycle to fifth cycle. Desorption efficiency also decreased marginally from 99.67% for first cycle to 94.25% for fifth cycle. Desorption efficiency of fifth cycle decreased only by 5.44% as compared to first cycle confirming very good reuse characteristics. The small decrease in the capacity can be attributed to possible loss of the active sites on the biosorbent. The obtained results indicated that NaOH activated FR biosorbent used in present study can be recovered and used repeatedly in treatment of dye containing wastewater without much loss in the efficiency.

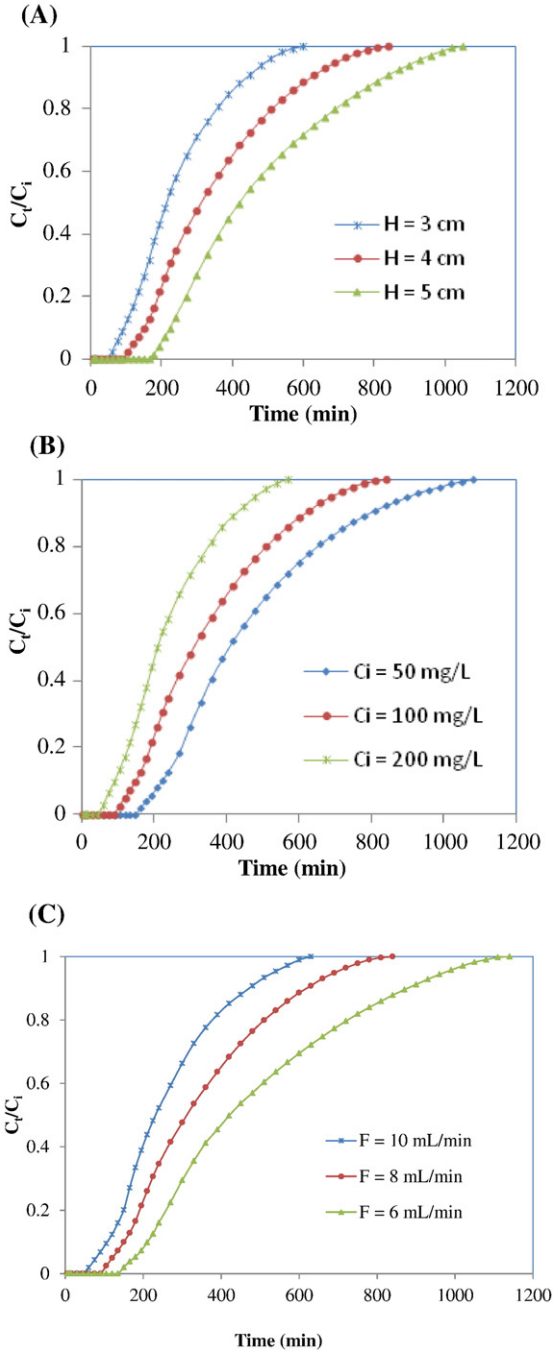

Fig. 9. Effect of operating parameters on breakthrough curve for biosorption of AV 17 dye on NaOH activated FR biosorbent A) bed height B) initial dye concentration C) flow rate.

Table 6
Breakthrough parameters at different bed height (H), initial dye concentration (C_i) and flow rate (F).

H (cm)	C_i (mg/L)	F (mL/min)	t_b (min)	t_e (min)	V_e (L)	q_{exp} (mg/g)
3	100	8	95	440	3.52	46.90
4	100	8	150	630	5.04	51.12
5	100	8	230	840	6.72	56.04
4	50	8	225	810	6.48	34.03
4	200	8	90	425	3.4	69.08
4	100	6	210	870	5.22	53.50
4	100	10	110	480	4.8	47.57

3.3. Column studies

3.3.1. Effect of biosorbent bed height (H)

The breakthrough curves obtained for biosorption of AV 17 on NaOH activated FR biosorbent at different biosorbent bed heights of 3, 4 and 5 cm at constant dye flow rate of 8 mL/min and initial dye concentration of 100 mg/L have been depicted in Fig. 9A. The obtained results for the design parameters are presented in Table 6. Breakthrough time is the important parameter deciding the column operation. Larger value of breakthrough time indicates higher biosorption capacity of the column. It can be seen from Table 6 that an increase in bed height from 3 to 5 cm increased the breakthrough time from 95 to 230 min. This could be attributed to the fact that with increase in bed height, contact time of dye inside the column is increased attributed to presence of higher quantum of material and higher residence time. Decrease in slope of the breakthrough curve was also observed with an increase in bed height. The biosorption capacity also increased from 46.9 to 56.04 mg/g with an increase in bed height from 3 to 5 cm. Higher biosorption capacity with an increase in bed height can be attributed to the fact that more quantity of the biosorbent is available at higher bed heights, which provides more contact time for adsorption of dye molecules on the biosorbent. Similar trends were also reported for the adsorption of Congo red on tea waste [61] and for the adsorption of orange II dye on bimetallic chitosan particles [62].

3.3.2. Effect of initial dye concentration (C_i)

The breakthrough curves obtained at different initial dye concentrations of 50, 100 and 200 mg/L at constant flow rate of 8 mL/min and bed height of 4 cm have been given in Fig. 9B and the obtained design parameter values are shown in Table 6. It is observed that when dye concentration was increased from 50 to 200 mg/L, treated effluent volume decreased from 6.48 to 3.4 L and breakthrough time decreased from 225 to 90 min. Better column performance at lower dye concentration is

Table 7
Thomas model parameters for removal of AV 17 using NaOH activated FR biosorbent.

H (cm)	Ci (mg/L)	F (mL/min)	k_{Th} (mL/min mg^{-1})	q_{Th} (mg/g)	q_m (mg/g)	R^2	SSE
3	100	8	0.136	48.28	46.90	0.9625	0.0026
4	100	8	0.100	52.79	51.12	0.9606	0.0027
5	100	8	0.079	58.06	56.04	0.9383	0.0034
4	50	8	0.158	35.75	34.03	0.9593	0.0033
4	200	8	0.068	70.93	69.08	0.9689	0.0023
4	100	6	0.072	55.75	53.50	0.9418	0.0038
4	100	10	0.127	49.91	47.57	0.9596	0.0031

Table 8
Adams–Bohart model parameters for removal of AV 17 using NaOH activated FR.

H (cm)	Ci (mg/L)	F (mL/min)	$k_{AB} \times 10^5$ (L/mg min^{-1})	N_0 (mg/L)	R^2	SSE
3	100	8	5.3	38,278.78	0.6978	0.1128
4	100	8	3.8	41,400.29	0.7148	0.088
5	100	8	3.2	42,435.38	0.6687	0.0785
4	50	8	6.4	26,376.89	0.6928	0.1175
4	200	8	2.8	54,324.00	0.7267	0.1158
4	100	6	2.9	41,680.94	0.6921	0.1063
4	100	10	5.5	37,583.63	0.7092	0.1433

observed as there is less competition for dye molecules to get adsorbed on the biosorbent surface at lower dye concentration as well as slower saturation of the bed occurs and hence increase in treated volume and breakthrough time was observed at lower dye concentration [63]. Increase in AV 17 dye concentration from 50 to 200 mg/L led to increase in biosorption capacity from 34.03 to 69.08 mg/g. This can be attributed to the fact that more driving force for mass transfer is available at higher initial dye concentration leading to an increase in biosorption capacity. Similar trends have been reported for the adsorption of Indosol Orange RSN on peanut husk [64] based biosorbent.

3.3.3. Effect of flow rate (F)

The breakthrough curves obtained at different flow rates of 6, 8 and 10 mL/min at constant dye concentration of 100 mg/L and biosorbent height of 4 cm have been given in Fig. 9C with the design parameters depicted in Table 6. It can be seen from Table 6 that when dye flow rate was increased from 6 to 10 mL/min, the breakthrough time was significantly decreased from 210 to 110 min. Biosorption capacity also decreased from 53.50 to 47.57 mg/g when flow rate was increased from 6 to 10 mL/min. At higher values of flow rate, time of contact of dye molecules in the column is not enough and dye leaves column before equilibrium is established, leading to decrease in breakthrough time and hence biosorption capacity. Similar variation trends were previously reported for the removal of textile red dye using adsorbents obtained from poly-functionalized pyroxene nanoparticles [65] and adsorption of Drimarine Black CL-B dye on lignocellulosic waste [66] based biosorbent.

3.3.4. Application of dynamic adsorption models to column performance data

In the present study, Thomas and Adams–Bohart models have been applied to predict breakthrough behavior in column system.

3.3.4.1. Thomas model: Thomas model [67] is the most widely used model to describe adsorption in continuous operation. The model assumes Langmuir kinetics and plug flow in the column. The model is expressed by following equation:

$$\frac{C_t}{C_i} = \frac{1}{1 + \exp\left(\frac{k_{Th} q_{Th} M}{F} - k_{Th} C_i t\right)} \tag{17}$$

Where k_{Th} is constant of Thomas model (mL/min mg^{-1}) and q_{Th} is equilibrium biosorption capacity (mg/g).

Thomas model was applied to the obtained experimental data and obtained model parameters (k_{Th} and q_{Th}) have been depicted in Table 7. It can be established from Table 7 that the values of biosorption capacity, q_{Th} increased and model constant, k_{Th} decreased with an increase in bed height and initial dye concentration and opposite trend was observed for an increase in flow rate. The obtained trend for Thomas parameter values indicated that lower flow rate and higher bed height favored adsorption of AV 17 dye on NaOH activated FR. At these optimized conditions of lower flow rate and higher bed height, residence time of dye solution in the biosorbent bed is estimated to be the maximum as 2.62 min and superficial velocity as 2.29 cm/min. Increase in q_{Th} at higher concentration is attributed to an increase in concentration driving force for mass transfer. Similar trends have also been reported for the removal of light green dye using surfactant modified peanut [68] and the adsorption of Indosol Yellow BG dye on peanut husk [69] based biosorbent and. It was also seen from Table 7 that correlation coefficient, R^2 values are quite close to unity and the maximum biosorption capacity found experimentally, q_m and calculated by Thomas model, q_{Th} are also closer to each other. The SSE values are also very less for all the studied parameters. All these findings confirmed better fitting of the Thomas model to the obtained column data.

3.3.4.2. Adams–Bohart model: Adams-Bohart model [70] assumes that adsorption rate is directly proportional to the concentration of adsorbing species and adsorbent residual capacity. The model is expressed by following equation:

$$\frac{C_t}{C_i} = \exp\left(k_{AB} C_i t - \frac{k_{AB} N_0 H}{U}\right) \tag{18}$$

Where k_{AB} is model rate constant (L/mg min^{-1}), N_0 is biosorption capacity (mg/L), H is biosorbent bed height (cm) and U is velocity of dye solution in the column (cm/min).

Adams-Bohart model was applied to the obtained experimental data and obtained model parameters (k_{AB} and N_0) have been depicted in Table 8. It was found that an increase in bed height and initial dye concentration led to decrease in k_{AB} and increase in N_0. However, it was seen from Table 8 that correlation coefficient, R^2 values are remarkably deviating from unity and SSE values are also more for all the experimental sets indicating that model does not fit the experimental data well.

3.3.5. Column regeneration studies

Regeneration of the spent adsorbent is important to establish the economic feasibility of the adsorption operation. Adsorption-desorption cycle studies were performed by first loading the column with 4 cm of NaOH activated FR bed and 100 mg/L of AV 17 dye solution passed in the upward direction through the column at the flow rate of 8 mL/min. After each adsorption step, biosorbent was regenerated in the column based on desorbing dye from biosorbent using the alkaline distilled water as an eluent. The eluent was passed through the column at a flow rate of 8 mL/min and desorption cycle was for 120 min. It was observed that for all 5 cycles of reuse for adsorption, dye removal at faster rate was observed in initial period of 15–30 min, though overall there was marginal decrease in the adsorption capacity. The results obtained for column regeneration study are depicted in Fig. 10. With reuse, the adsorption capacity decreased from 50.87 mg/g for first cycle to 46.03 mg/g for fifth cycle (about 10% reduction). Desorption

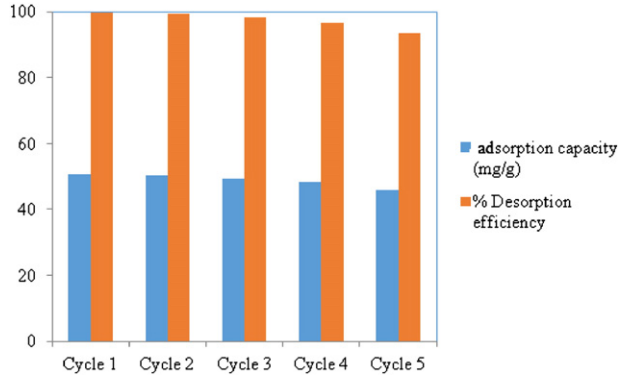

Fig. 10. Regeneration of NaOH activated FR biosorbent and performance for five cycles in column study.

efficiency also decreased from 99.52% to 93.54%. The obtained results indicated that spent NaOH activated FR could be regenerated in a column and reused for dye adsorption effectively for 5 cycles with marginal reduction in the capacity. Regeneration results confirmed economic feasibility of the biosorbent used in present study.

4. Conclusions

The present study highlighted the potential of NaOH activated *Ficus racemosa* fallen leaves, a waste biomass giving significant biosorption capacity for the adsorptive removal of acid violet 17 dye from wastewater. Maximum biosorption capacity established in the batch study was 119.05 mg/g at pH 2 and 3 g/L of biosorbent dose, which was found to be substantially higher as compared to the commonly used biosorbents. The obtained kinetic data was in good agreement with pseudo second-order model and isotherm data suitably fitted to Langmuir isotherm. The observed design parameters for the column study were in good agreement with Thomson model. Desorption study performed for batch as well as column study established the potential of synthesized biosorbent to be used repeatedly to treat dye effluents.

Acknowledgements

The authors acknowledge University Grant Commission for assistance under UGC Networking Resource Centre, at the Institute of Chemical Technology, Mumbai, India.

References

[1] V.S. Munagapati, D. Kim, Adsorption of anionic azo dye Congo red from aqueous solution by cationic modified Orange peel powder, J. Mol. Liq. 220 (2016) 540–548.
[2] B. Mu, A. Wang, Adsorption of dyes onto palygorskite and its composites: a review, J. Environ. Chem. Eng. 4 (2016) 1274–1294.
[3] S. Farhadi, M.M. Amini, M. Dusek, M. Kucerakova, F. Mahmoudi, A new nanohybrid material constructed from Keggin-type polyoxometalate and Cd (II) semicarbazone Schiff base complex with excellent adsorption properties for the removal of cationic dye pollutants, J. Mol. Struct. 1130 (2017) 592–602.
[4] R. Ahmad, R. Kumar, Adsorptive removal of congo red dye from aqueous solution using bael shell carbon, Appl. Surf. Sci. 257 (2010) 1628–1633.
[5] A. Roy, S. Chakraborty, S.P. Kundu, B. Adhikari, S.B. Majumder, Adsorption of anionic-azo dye from aqueous solution by lignocellulose-biomass jute fiber: equilibrium, kinetics, and thermodynamics study, Ind. Eng. Chem. Res. 51 (2012) 12095–12106.
[6] G.G. Sonai, S.M.A.G.U. De Souza, D. de Oliveira, A.A.U. de Souza, The application of textile sludge adsorbents for the removal of Reactive Red 2 dye, J. Environ. Manag. 168 (2016) 149–156.
[7] N. Belhouchat, H. Zaghouane-Boudiaf, C. Viseras, Removal of anionic and cationic dyes from aqueous solution with activated organo-bentonite/sodium alginate encapsulated beads, Appl. Clay Sci. 135 (2017) 9–15.
[8] V. da S. Lacerda, J.B. Lopez-Sotelo, A. Correa-Guimares, S. Hernandez-Navarro, M. Sanchez-Bascones, L.M. Navas-Gracia, P. Martín-Ramos, J. Martín-Gil, Rhodamine B removal with activated carbons obtained from lignocellulosic waste, J. Environ. Manag. 155 (2015) 67–76.
[9] Y. Zhou, L. Zhang, Z. Cheng, Removal of organic pollutants from aqueous solution using agricultural wastes: a review, J. Mol. Liq. 212 (2015) 739–762.
[10] C.A.P. Almeida, A. dos Santos, S. Jaerger, N.A. Debacher, N.P. Hankins, Mineral waste from coal mining for removal of astrazon red dye from aqueous solutions, Desalination 264 (2010) 181–187.
[11] S.V. Mohan, N.C. Rao, J. Karthikeyan, Adsorptive removal of direct azo dye from aqueous phase onto coal based sorbents: a kinetic and mechanistic study, J. Hazard. Mater. 90 (2002) 189–204.
[12] G.Y. Fu, T. Viraraghavan, Removal of disperse red 1 from an aqueous solution by fungus aspergillus niger, Desalin. Water Treat. 25 (2011) 187–194.
[13] Y. Fu, T. Viraraghavan, Removal of C.I. acid blue 29 from an aqueous solution by Aspergillus niger, Am. Assoc. Text. Chem. Color. Rev. 1 (2001) 36–40.
[14] Y. Fu, T.U. Viraraghavan, Removal of Congo red from an aqueous solution by fungus aspergillus niger, Adv. Environ. Res. 7 (2002) 239–247.
[15] S.N. Jain, P.R. Gogate, NaOH-treated dead leaves of *Ficus racemosa* as an efficient biosorbent for acid blue 25 removal, Int. J. Environ. Sci. Technol. 14 (2017) 531–542.
[16] A. Faki, M. Turan, O. Ozdemir, A.Z. Turan, Analysis of fixed-bed column adsorption of reactive yellow 176 onto surfactant-modified zeolite, Ind. Eng. Chem. Res. 47 (2008) 6999–7004.
[17] M.A. Martin-Lara, G. Blazquez, A. Ronda, I.L. Rodriguez, M. Calero, Multiple biosorption–desorption cycles in a fixed-bed column for Pb (II) removal by acid-treated olive stone, J. Ind. Eng. Chem. 18 (2012) 1006–1012.
[18] M. Auta, B.H. Hameed, Chitosan – clay composite as highly effective and low-cost adsorbent for batch and fixed-bed adsorption of methylene blue, Chem. Eng. J. 237 (2014) 352–361.
[19] S. Amirnia, M.B. Ray, A. Margaritis, Copper ion removal by Acer saccharum leaves in a regenerable continuous-flow column, Chem. Eng. J. 287 (2016) 755–764.
[20] R. Han, Y. Wang, X. Zhao, Y. Wang, F. Xie, J. Cheng, M. Tang, Adsorption of methylene blue by phoenix tree leaf powder in a fixed-bed column: experiments and prediction of breakthrough curves, Desalination 245 (2009) 284–297.
[21] M. Kousha, E. Daneshvar, M.S. Sohrabi, M. Jokar, A. Bhatnagar, Adsorption of acid orange II dye by raw and chemically modified brown macroalga Stoechospermum marginatum, Chem. Eng. J. 192 (2012) 67–76.
[22] M. Yu, J. Li, L. Wang, KOH-activated carbon aerogels derived from sodium carboxymethyl cellulose for high-performance supercapacitors and dye adsorption, Chem. Eng. J. 310 (2017) 300–306.
[23] E.F. Lessa, M.S. Gularte, E.S. Garcia, A.R. Fajardo, Orange waste: a valuable carbohydrate source for the development of beads with enhanced adsorption properties for cationic dyes, Carbohydr. Polym. 157 (2017) 660–668.
[24] Y. Li, A. Meas, S. Shan, R. Yang, X. Gai, Production and optimization of bamboo hydrochars for adsorption of Congo red and 2-naphthol, Bioresour. Technol. 207 (2016) 379–386.
[25] P. Jha, R. Jobby, N.S. Desai, Remediation of textile azo dye acid red 114 by hairy roots of *Ipomoea carnea* Jacq. and assessment of degraded dye toxicity with human keratinocyte cell line, J. Hazard. Mater. 311 (2016) 158–167.
[26] M. Malakootian, H.J. Mansoorian, A. Hosseini, N. Khanjani, Evaluating the efficacy of alumina/carbon nanotube hybrid adsorbents in removing azo reactive red 198 and blue 19 dyes from aqueous solutions, Process. Saf. Environ. Prot. 96 (2015) 125–137.
[27] T.L. Silva, A. Ronix, O. Pezoti, L.S. Souza, P.K.T. Leandro, K.C. Bedin, K.K. Beltrame, A.L. Cazetta, V.C. Almeida, Mesoporous activated carbon from industrial laundry sewage sludge: adsorption studies of reactive dye Remazol brilliant blue R, Chem. Eng. J. 303 (2016) 467–476.
[28] S.P.D.M. Blanco, F.B. Scheufele, A.N. Módenes, F.R. Espinoza-Quiñones, P. Marin, A.D. Kroumov, C.E. Borb, Kinetic, equilibrium and thermodynamic phenomenological modeling of reactive dye adsorption onto polymeric adsorbent, Chem. Eng. J. 307 (2017) 466–475.
[29] R. Lafi, A. Hafiane, Removal of methyl orange (MO) from aqueous solution using cationic surfactants modified coffee waste (MCWs), J. Taiwan Inst. Chem. Eng. 58 (2016) 424–433.
[30] N.F. Cardoso, E.C. Lima, I.S. Pinto, C.V. Amavisca, B. Royer, R.B. Pinto, W.S. Alencar, S.F.P. Pereira, Application of cupuassu shell as biosorbent for the removal of textile dyes from aqueous solution, J. Environ. Manag. 92 (2011) 1237–1247.
[31] H.J. Kumari, P. Krishnamoorthy, T.K. Arumugam, S. Radhakrishnan, D. Vasudevan, An efficient removal of crystal violet dye from waste water by adsorption onto TLAC/chitosan composite: a novel low cost adsorbent, Int. J. Biol. Macromol. 96 (2017) 324–333.
[32] K. Rasool, D.S. Lee, Characteristics, kinetics and thermodynamics of Congo red biosorption by activated sulfidogenic sludge from an aqueous solution, Int. J. Environ. Sci. Technol. 12 (2013) 571–580.
[33] S.N. Jain, P.R. Gogate, Acid blue 113 removal from aqueous solution using novel biosorbent based on NaOH treated and surfactant modified fallen leaves of *Prunus Dulcis*, J. Environ. Chem. Eng. 5 (2017) 3384–3394.
[34] A. Salama, New sustainable hybrid material as adsorbent for dye removal from aqueous solutions, J. Colloid Interface Sci. 487 (2017) 348–353.
[35] G. Akkaya, F. Güzel, Application of some domestic wastes as new low-cost biosorbents for removal of methylene blue: kinetic and equilibrium studies, Chem. Eng. Commun. 201 (2014) 557–578.
[36] E.S.Z. El Ashtoukhy, Loofa egyptiaca as a novel adsorbent for removal of direct blue dye from aqueous solution, J. Environ. Manag. 90 (2009) 2755–2761.
[37] S. Lagergren, About the theory of so called adsorption of soluble substances, Ksver Veterskapsakad Handl. 24 (1898) 1–6.
[38] Y.S. Ho, G. Mckay, Pseudo-second order model for sorption processes, Process Biochem. 34 (1999) 451–465.
[39] Z. Belala, M. Jeguirim, M. Belhachemi, F. Addoun, G. Trouvé, Biosorption of basic dye from aqueous solutions by date stones and palm-trees waste: kinetic, equilibrium and thermodynamic studies, Desalination 271 (2011) 80–87.
[40] S. Chan, Y.P. Tan, A.H. Abdullah, S. Ong, Equilibrium, kinetic and thermodynamic studies of a new potential biosorbent for the removal of basic blue 3 and Congo red dyes: pineapple (Ananas Comosus) plant stem, J. Taiwan Inst. Chem. Eng. 61 (2016) 306–315.
[41] M. Auta, B.H. Hameed, Preparation of waste tea activated carbon using potassium acetate as an activating agent for adsorption of acid blue 25 dye, Chem. Eng. J. 171 (2011) 502–509.
[42] S.K. Theydan, M.J. Ahmed, Adsorption of methylene blue onto biomass-based activated carbon by $FeCl_3$ activation: equilibrium, kinetics, and thermodynamic studies, J. Anal. Appl. Pyrolysis 97 (2012) 116–122.
[43] Z. Jia, Z. Li, T. Ni, S. Li, Adsorption of low-cost absorption materials based on biomass (Cortaderia selloana flower spikes) for dye removal: kinetics, isotherms and thermodynamic studies, J. Mol. Liq. 229 (2017) 285–292.
[44] M.P. Tavlieva, S.D. Genieva, V.G. Georgieva, L.T. Vlaev, Kinetic study of brilliant green adsorption from aqueous solution onto white rice husk ash, J. Colloid Interface Sci. 409 (2013) 112–122.
[45] W.J. Weber, J. Carrell Morris, Kinetics of adsorption on carbon from solution, J. Sanit. Eng. Div. 89 (1963) 31–60.
[46] M. Arami, N.Y. Limaee, N.M. Mahmoodi, Evaluation of the adsorption kinetics and equilibrium for the potential removal of acid dyes using a biosorbent, Chem. Eng. J. 139 (2008) 2–10.
[47] R. Gong, S. Zhu, D. Zhang, J. Chen, S. Ni, R. Guan, Adsorption behavior of cationic dyes on citric acid esterifying wheat straw: kinetic and thermodynamic profile, Desalination 230 (2008) 220–228.

[48] A.B. Albadarin, M.N. Collins, M. Naushad, S. Shirazian, G. Walker, C. Mangwand, Activated lignin-chitosan extruded blends for efficient adsorption of methylene blue, Chem. Eng. J. 307 (2017) 264–272.
[49] N. Kannan, M.M. Sundaram, Kinetics and mechanism of removal of methylene blue by adsorption on various carbons — a comparative study, Dyes Pigments 51 (2001) 25–40.
[50] F. Kooli, Y. Liu, R. Al-faze, A. Al Suhaimi, Effect of acid activation of Saudi local clay mineral on removal properties of basic blue 41 from an aqueous solution, Appl. Clay Sci. 116–117 (2015) 23–30.
[51] Y. Zhang, J. Li, J. Zhao, W. Bian, Y. Li, X. Wang, Adsorption behavior of modified iron stick yam skin with Polyethyleneimine as a potential biosorbent for the removal of anionic dyes in single and ternary systems at low temperature, Bioresour. Technol. 222 (2016) 285–293.
[52] V.K. Gupta, S. Agarwal, A. Olgun, H.I. Demir, M.L. Yola, N. Atar, Adsorptive properties of molasses modified boron enrichment waste based nanoclay for removal of basic dyes, J. Ind. Eng. Chem. 34 (2016) 244–249.
[53] I. Langmuir, The adsorption of gases on plane surfaces of glass, mica and platinum, J. Am. Chem. Soc. 40 (1918) 1361–1403.
[54] M.M. Dubinin, L.V. Radushkevich, The equation of the characteristic curve of the activated charcoal, Chem. Zentralbl. 1 (1947) 875.
[55] M.J. Temkin, V. Pyzhev, Recent modifications to Langmuir isotherms, Acta Physicochim. USSR. 12 (1940) 217–225.
[56] S. Saber-samandari, S. Saber-samandari, H. Yekta, M. Mohseni, Adsorption of anionic and cationic dyes from aqueous solution using gelatin-based magnetic nanocomposite beads comprising carboxylic acid functionalized carbon nanotube, Chem. Eng. J. 308 (2017) 1133–1144.
[57] A. Bhatnagar, E. Kumar, A.K. Minocha, B. Jeon, H. Song, Y. Seo, Removal of anionic dyes from water using Citrus Limonum (lemon) peel: equilibrium studies and kinetic modeling, Sep. Sci. Technol. 44 (2009) 316–334.
[58] L. Lu, L. Jia, D.H.L. Ng, P. Yang, P. Song, M. Zuo, Synthesis of novel hierarchically porous Fe_3O_4@MgAl-LDH magnetic microspheres and its superb adsorption properties of dye from water, J. Ind. Eng. Chem. 46 (2017) 315–323.
[59] C. Wu, Adsorption of reactive dye onto carbon nanotubes: equilibrium, kinetics and thermodynamics, J. Hazard. Mater. 144 (2007) 93–100.
[60] A. Celekli, G. Ilgün, H. Bozkurt, Sorption equilibrium, kinetic, thermodynamic, and desorption studies of reactive red 120 on Chara contraria, Chem. Eng. J. 191 (2012) 228–235.
[61] M. Foroughi-dahr, M. Esmaieli, H. Abolghasemi, A. Shojamoradi, E.S. Pouya, Continuous adsorption study of congo red using tea waste in a fixed-bed column, Desalin. Water Treat. 57 (2016) 8437–8446.
[62] B. Ramavandi, S. Farjadfard, M. Ardjmand, Mitigation of orange II dye from simulated and actual wastewater using bimetallic chitosan particles: continuous flow fixed-bed reactor, J. Environ. Chem. Eng. 2 (2014) 1776–1784.
[63] Y.S. Al-degs, M.A.M. Khraisheh, S.J. Allen, M.N. Ahmad, Adsorption characteristics of reactive dyes in columns of activated carbon, J. Hazard. Mater. 165 (2009) 944–949.
[64] S. Sadaf, H.N. Bhatti, Evaluation of peanut husk as a novel, low cost biosorbent for the removal of Indosol Orange RSN dye from aqueous solutions: batch and fixed bed studies, Clean Techn. Environ. Policy 16 (2014) 527–544.
[65] A. Hethnawi, N.N. Nassar, A.D. Manasrah, G. Vitale, Poly(ethylenimine)-functionalized pyroxene nanoparticles embedded on diatomite for adsorptive removal of dye from textile wastewater in a fixed-bed column, Chem. Eng. J. 320 (2017) 389–404.
[66] S. Noreen, H.N. Bhatti, S. Nausheen, S. Sadaf, M. Ashfaq, Batch and fixed bed adsorption study for the removal of Drimarine black CL-B dye from aqueous solution using a lignocellulosic waste: a cost affective adsorbent, Ind. Crop. Prod. 50 (2013) 568–579.
[67] H.C. Thomas, Heterogeneous ion exchange in a flowing system, J. Am. Chem. Soc. 66 (1944) 1664–1666.
[68] T. Zhou, W. Lu, L. Liu, H. Zhu, Y. Jiao, S. Zhang, R. Han, Effective adsorption of light green anionic dye from solution by CPB modified peanut in column mode, J. Mol. Liq. 211 (2015) 909–914.
[69] S. Sadaf, H.N. Bhatti, Batch and fixed bed column studies for the removal of Indosol yellow BG dye by peanut husk, J. Taiwan Inst. Chem. Eng. 45 (2014) 541–553.
[70] G.S. Bohart, E.Q. Adams, Some aspects of the behavior of charcoal with respect to chlorine, J. Am. Chem. Soc. 42 (1920) 523–544.
[71] R. Sivaraj, C. Namasivayam, K. Kadirvelu, Orange peel as an adsorbent in the removal of acid violet 17 (acid dye) from aqueous solutions, Waste Manag. 21 (2001) 105–110.
[72] M.R.R. Kooh, M.K. Dahri, L.B.L. Lim, L.H. Lim, Batch adsorption studies on the removal of acid blue 25 from aqueous solution using Azolla pinnata and soya bean waste, Arab. J. Sci. Eng. 41 (2016) 2453–2464.
[73] V. Hernández-montoya, D.I. Mendoza-castillo, A. Bonilla-petriciolet, M.A. Montes-Morán, M.A. Pérez-Cruz, Role of the pericarp of Carya illinoinensis as biosorbent and as precursor of activated carbon for the removal of lead and acid blue 25 in aqueous solutions, J. Anal. Appl. Pyrolysis 92 (2011) 143–151.
[74] N. Atar, A. Olgun, Removal of acid blue 062 on aqueous solution using calcinated colemanite ore waste, J. Hazard. Mater. 146 (2007) 171–179.
[75] D. Robati, B. Mirza, M. Rajabi, O. Moradi, I. Tyagi, S. Agarwal, V.K. Gupta, Removal of hazardous dyes-BR 12 and methyl orange using graphene oxide as an adsorbent from aqueous phase, Chem. Eng. J. 284 (2015) 687–697.
[76] V.K. Gupta, D. Pathania, S. Sharma, S. Agarwal, P. Singh, Remediation and recovery of methyl orange from aqueous solution onto acrylic acid grafted Ficus carica fiber: isotherms, kinetics and thermodynamics, J. Mol. Liq. 177 (2013) 325–334.
[77] L.D. Fiorentin, D.E.G. Trigueros, A.N. Módenes, F.R. Espinoza-qui, N.C. Pereira, S.T.D. Barros, O.A.A. Santos, Biosorption of reactive blue 5G dye onto drying orange bagasse in batch system: kinetic and equilibrium modeling, Chem. Eng. J. 163 (2010) 68–77.
[78] E. Alver, A.Ü. Metin, Anionic dye removal from aqueous solutions using modified zeolite: adsorption kinetics and isotherm studies, Chem. Eng. J. 202 (2012) 59–67.
[79] E.Y. Ozmen, M. Yilmaz, Use of β-cyclodextrin and starch based polymers for sorption of Congo red from aqueous solutionss, J. Hazard. Mater. 148 (2007) 303–310.
[80] C. Namasivayam, D. Kavitha, Removal of Congo red from water by adsorption onto activated carbon prepared from coir pith, an agricultural solid waste, Dyes Pigments 54 (2002) 47–58.